BAROCLINIC INSTABILITY OF BOTTOM-DWELLING CURRENTS

MATEUSZ K. RESZKA AND GORDON E. SWATERS
Applied Mathematics Institute
Department of Mathematical Sciences
University of Alberta
Edmonton, Alberta, Canada

1. Introduction

Density-driven benthic flows are important in the dynamics of marginal seas, river estuaries and other coastal regions (LeBlond *et al.*, 1991; Price & O'Neil Baringer, 1994). They often occur along sloping continental shelves, flowing with shallower water on their right (in the northern hemisphere). Mesoscale gravity currents, which are to be discussed in this study, arise from a geostrophic balance between down-slope acceleration due to gravity and the Coriolis force, while their dynamics is characterized by lengthscales on the order of the Rossby deformation radius. There is mounting evidence that such flows are subject to instability, which may drastically alter the mean flow and culminate in a series of isolated plumes or eddies (Armi & D'Asaro, 1980; Houghton *et al.*, 1982).

While previous modelling studies often employed the streamtube approximation (Smith, 1975) or the full primitive equations (Jiang & Garwood Jr., 1995), here we present preliminary numerical results using a two layer, frontal geostrophic model (Poulin & Swaters, 1999). The model allows for continuous stratification in the upper layer and relies on the release of gravitational potential energy due to the gradual downslope slumping of the dense fluid. We investigate the nonlinear spatio-temporal evolution of a baroclinically unstable gravity current on a linearly sloping bottom. The model is also applied to fluctuating deep currents in the Strait of Georgia (located between Vancouver Island and mainland British Columbia, Canada), as described in Stacey *et al.* (1988). The reader is referred to Reszka & Swaters, (2000) for a more thorough examination of the above results.

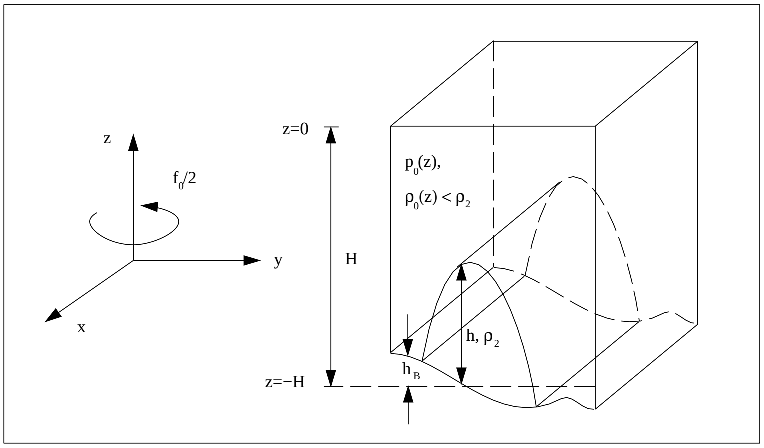

Figure 1. Geometry of the frontal geostrophic model. The upper layer is continuously stratified and the interface is allowed to intersect the topography.

2. Governing Equations

The present model assumes a continuously stratified layer of finite depth overlying a dense, homogeneous layer and sloping (or otherwise varying) bottom topography. The interface between the two layers can intersect the topography (see fig. 1), allowing for isolated patches of dense fluid. The governing equations are derived in an asymptotic expansion of the shallow water equations for the lower layer and the Boussinesq equations for the upper layer. We refer the reader to Poulin & Swaters (1999) for details. The leading order non-dimensional fields on an f-plane are determined by

$$(\Delta\varphi + (N^{-2}\varphi_z)_z)_t + \mu J(\varphi, \Delta\varphi + (N^{-2}\varphi_z)_z) = 0, \tag{1}$$

$$\varphi_{zt} + \mu J(\varphi, \varphi_z) = 0, \qquad z = 0, \tag{2}$$

$$\varphi_{zt} + \mu J(\varphi, \varphi_z) + N^2 J(\varphi + h, h_B) = 0, \qquad z = -1, \tag{3}$$

$$h_t + J(\mu\varphi + h_B, h) = 0, \qquad z = -1, \tag{4}$$

where $\varphi(x, y, z, t)$ is the upper layer geostrophic pressure, $h(x, y, t)$ is the lower layer thickness, $h_B(x, y)$ is the height of the bottom topography, $J(A, B) = A_x B_y - B_x A_y$ and subscripts refer to derivatives unless otherwise specified. Here N is a scaled Brunt-Väisälä frequency while μ is referred to as the interaction parameter and measures the destabilizing effect of baroclinicity relative to the stabilizing influence of topography. In order to gain insight into the basic instability mechanism we assume a simple model configuration, i.e. constant stratification in the upper layer ($N = const.$) and an x-invariant bottom topography ($h_B = h_B(y)$).

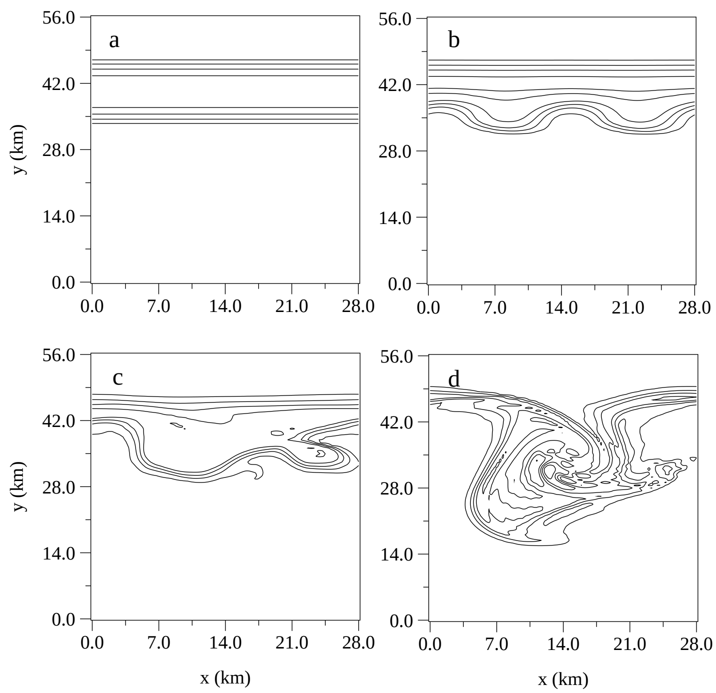

Figure 2. Evolution of lower layer height, h, at a) 0, b) 7, c) 10 and d) 12 days for linearly sloping topography. Contour range is 0–60 m with a contour interval of 15 m.

3. Numerical Solutions

Initially an x-invariant, parabolic profile was specified for the lower layer height. Its half-width was equal to the Rossby radius associated with the upper layer, while its maximum thickness was approximately 10% of the total fluid depth. The upper layer initially consisted of a small-amplitude, random wavefield, which served to excite the instability. The system was integrated forward in time in an x-periodic channel with the no-normal flow boundary condition at the walls. The length of the channel was chosen such that it allowed two or three wavelengths of the most unstable mode. The domain was typically discretized into $120\times120\times16$ grid nodes, yielding a dimensional resolution of roughly 230 m in the horizontal and 24 m in the vertical.

A simulation with a linearly sloping bottom was performed first. While this is a crude approximation of a continental shelf, it isolates the process of instability we wish to study from additional topographic effects. The evolution of the lower layer thickness for this simulation is given in fig. 2 at day a) 0, b) 7, c) 10 and d) 12. At 7 days the instability is manifested

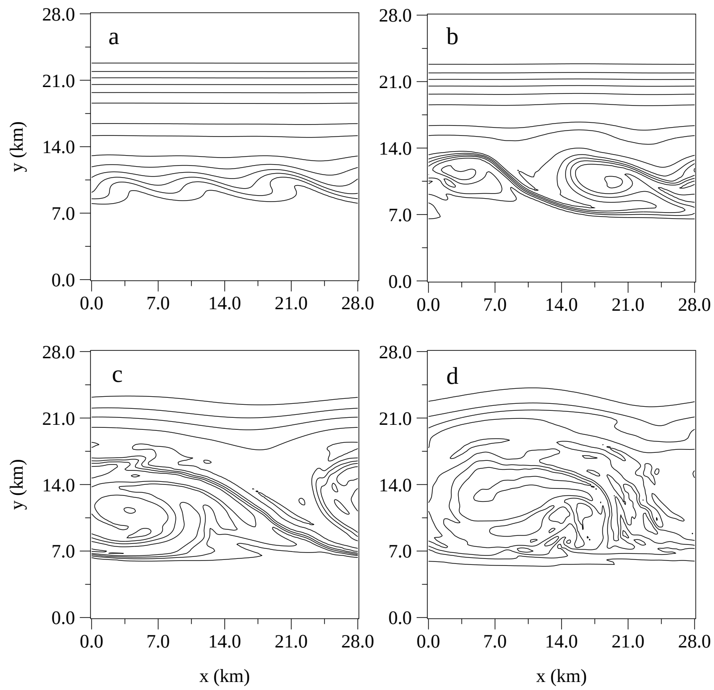

Figure 3. Evolution of lower layer height, h, at a) 8, b) 10, c) 12 and d) 14 days for Strait of Georgia topography. Contour range is 0–60 m with a contour interval of 10 m.

as a growing, periodic deformation of the incropping on the downslope side of the current (the fluid column deepens in the negative y-direction). We estimate e-folding times of about 11 hours and a phase speed of 12 cm/s. The primary source of energy for the growth of perturbations is the potential energy released as the dense fluid slowly descends down the slope (Reszka & Swaters, 2000). The two waves initially seen in the channel then decay and merge into one at 10 days. This longer mode grows until the wave breaks backwards, relative to the direction of the current, and begins to roll up on itself. This process eventually destroys the mean flow (day 12) and results in a coherent patch of dense fluid which rotates anticyclonically.

We note that this simulation was repeated in a channel with twice the length, yielding similar results both qualitatively and quantitatively. The spiral-like cold domes we obtained are similar to the ones observed by Swaters (1998) for a two layer, frontal geostrophic model with homogeneous upper layer (Swaters, 1991). However, the dominant lengthscales associated with the continuously stratified model are invariably smaller (Poulin & Swaters, 1999; Reszka & Swaters, 2000).

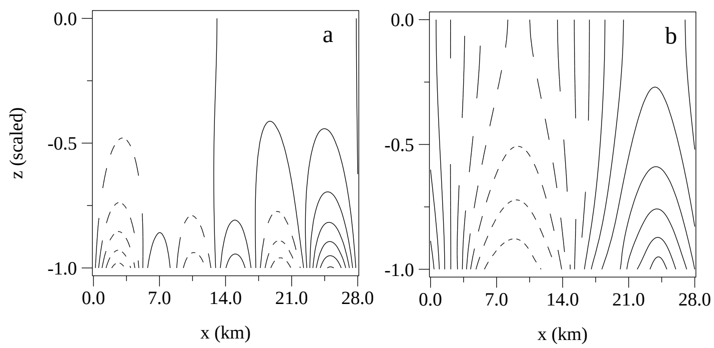

Figure 4. Vertical cross-sections of the nondimensional upper layer pressure at y = 10 km, corresponding to fig. 3a and 3d. Dashed contours correspond to negative values.

The second simulation we present employs bottom topography appropriate for the Strait of Georgia. The topography is comprised of a y-dependent sinusoidal function which forms a trough. Initially, the current rests entirely on one slope of this trough. Low frequency variability within the Strait of Georgia has been attributed to fluctuations and instability of deep currents which propagate along the coast (see LeBlond *et al.*, 1991; Stacey *et al.*, 1988). Fig. 3 depicts four contour plots of the lower layer thickness for this simulation at day a) 8, b) 10, c) 12 and d) 14. In fig. 3a we again see the wavelike deformation of the downslope incropping. It is noteworthy that the fastest-growing wavenumber is about three times the one predicted for the Swaters (1991) model (see Karsten *et al.*, 1995). The e-folding time for this phase of instability is quite short, approximately 7 h. The perturbation moves with the current (i.e. in the negative x-direction) at a speed of roughly 7 cm/s. As the deformations grow, they subsequently encounter the opposite face of the trough ($y < 7$ km) which induces a velocity in the positive x-direction. This, in effect, accelerates the merging of the modes into one anticyclonic gyre which encompasses most of the channel domain (fig. 3c). By 14 days the flow reaches a quasi-steady state (fig. 3d), exhibiting many small-scale filamentous structures.

4. Discussion

In both simulations a train of alternating cyclonic and anticyclonic eddies emerges in the upper layer streamfunction as the instability progresses. These eddies quickly attain a tapered, bottom-intensified shape. Vertical cross-sections of the upper layer pressure at $y = 10$ km are given in fig. 4. Figures 4a and 4b correspond to day 8 and 14, respectively, of the Strait of

Georgia simulation (see fig. 3a and 3d). This vertical structure is consistent with the analysis of Stacey *et al.* (1988) who found evidence of several bottom-intensified vortices in the strait. Surface signatures of deep eddies have also been reported in association with the Denmark Strait Overflow (Bruce, 1995). If such vortices are the result of baroclinic instability, then the present model may provide an appropriate mathematical framework for the dynamics of deep water masses leaving the Denmark Strait.

Acknowledgments: Preparation of this manuscript was supported in part by a PGS A grant awarded to M. K. R. by the Natural Sciences and Engineering Research Council of Canada, a Graduate Fellowship awarded to M. K. R. by the University of Alberta, as well as a research grant awarded to G. E. S. by the Natural Sciences and Engineering Research Council of Canada. A travel grant was also awarded to M. K. R. by the Institute for Geophysical Research.
Author's e-mail: mreszka@acubens.math.ualberta.ca,
WWW address: fluids.math.ualberta.ca/~mreszka/

References

Armi, L. & D'Asaro, E. (1980) Flow structures of the benthic ocean. *J. Geophys. Res.* **85**, 469–484.

Bruce, J. G. (1995) Eddies southwest of the Denmark Strait. *Deep-Sea Research* **42**, 13–29.

Houghton, R. W., Schlitz, R., Beardsley, R. C., Butman, B. & Chamberlin, J. L. (1982) The Middle Atlantic Bight Cold Pool: Evolution of the Temperature Structure During Summer 1979. *J. Phys. Oceanogr.* **12**, 1019–1029.

Jiang, L. & Garwood Jr., R. W. (1995) A numerical study of three-dimensional dense bottom plumes on a Southern Ocean continental slope. *J. Geophys. Res.* **100**, 18,471–18,488.

Karsten, R. H., Swaters, G. E. & Thomson, R. E. (1995) Stability Characteristics of Deep-Water Replacement in the Strait of Georgia. *J. Phys. Oceanogr.* **25**, 2391–2403.

LeBlond, P. H., Ma, H., Doherty, F. & Pond, S. (1991) Deep and Intermediate Water Replacement in the Strait of Georgia. *Atmos.-Ocean* **29**, 288–312.

Poulin, F. J. & Swaters, G. E. (1999) Sub-inertial dynamics of density-driven flows in a continuously stratified fluid on a sloping bottom. I. Model derivation and stability characteristics. *Proc. R. Soc. Lond. A* **455**, 2281–2304.

Price, J. F. & O'Neil Baringer, M. (1994) Outflows and deep water production by marginal seas. *Prog. Oceanog.* **33**, 161–200.

Reszka, M. K. & Swaters, G. E. (2000) Baroclinic instability of benthic currents in a continuously stratified ocean. Submitted to *Can. App. Math. Quart.*

Smith, P. C. (1975) A streamtube model for bottom boundary currents in the ocean. *Deep-Sea Res.* **22**, 853–873.

Stacey, J. W., Pond, S. & LeBlond, P. H. (1988) An objective analysis of the low-frequency currents in the Strait of Georgia. *Atmos.-Ocean* **26**, 1–15.

Swaters, G. E. (1991) On the baroclinic instability of cold-core coupled density fronts on a sloping continental shelf. *J. Fluid Mech.* **224**, 361–382.

Swaters, G. E. (1998) Numerical simulations of the baroclinic dynamics of density-driven coupled fronts and eddies on a sloping bottom. *J. Geophys. Res.* **103**, 2945–2961.